Journal of Power Sources 196 (2011) 620–626

Contents lists available at ScienceDirect

Journal of Power Sources

journal homepage: www.elsevier.com/locate/jpowsour

Effect, mechanism and recovery of nitrogen oxides poisoning on oxygen reduction reaction at Pt/C catalysts

Meng Chen [a,*], Chunyu Du [b,**], Jing Zhang [a], Panpan Wang [b], Tong Zhu [b]

[a] College of Materials Science and Chemical Engineering, Harbin Engineering University, Harbin 150001, China
[b] School of Chemical Engineering and Technology, Harbin Institute of Technology, Harbin 150001, China

ARTICLE INFO

Article history:
Received 22 June 2010
Received in revised form 29 July 2010
Accepted 29 July 2010
Available online 7 August 2010

Keywords:
Fuel cell
Nitrogen oxides
Impurity poisoning
Oxygen reduction reaction
Pt catalyst

ABSTRACT

The poisoning of nitrogen oxides (NO_x) on the oxygen reduction reaction (ORR) at the Pt/C catalyst has been studied for proton exchange membrane fuel cells by a three-electrode method in liquid electrolyte solution. The cyclic voltammetry (CV) results reveal that the absorption of NO_x on metallic Pt is more significant than on Pt oxides, and this absorption is probably a chemical rather than an electrochemical process. Linear sweeping voltammetry (LSV) curves for the ORR show that it is the absorption of NO_x on the Pt surface that results in significant performance degradation of Pt/C catalysts. This degradation is mainly due to the reduction of electrochemically active surface area, since the ORR mechanism remains almost the same after the NO_x poisoning as revealed by similar Tafel slopes. Because lower potentials facilitate the reduction of NO_x to water soluble NH_4^+, reducing the working potential can mitigate the poisoning of NO_x. However, to completely recover the performance loss due to NO_x poisoning through the potential sweeping, it is found that the oxidation removal is more efficient than the reduction removal.

1. Introduction

The proton exchange membrane (PEM) fuel cell has been the subject of intensive research, owing to its low operating temperature, fast start-up, high efficiency and zero emissions. Before it becomes viable for large-scale applications, however, significant challenges have to be addressed. Among them, degradation of the platinum (Pt) catalyst has been reported to be a major one because it is closely associated with the life-time of PEM fuel cell [1]. Currently, the PEM fuel cell often uses air as oxidant, so that it is inevitable that the contaminants in the air, such as NO_x, SO_x and hydrocarbons, can be introduced into the cathode of fuel cell. These contaminants have recently been identified to be one of the significant factors that contribute to the catalyst degradation [1–3].

Nitrogen oxides (NO_x), which mainly come from automotive vehicle exhausts and industrial manufacturing processes, are major contaminants present in the air. So far, several studies concerning the poisoning of NO_x on the performance of PEM fuel cell have been reported [2,4–9]. Moore et al. [4] and Nagahara et al. [2] demonstrated that the poisoning of a low concentration NO_2 on fuel cell was almost negligible. In contrast, the results of Mohtadi et al. [5] and Jing et al. [6] indicated that the intrusion of NO_2 quickly degraded fuel cell performance, and this degradation could even reach 50% of the initial performance. As to the poisoning mechanism of NO_x, some results suggested that it was related to the adsorption of NO_x on the catalyst surface [6]. For example, Knights et al. [7] used cyclic voltammetry (CV) to identify the adsorption of NO_x on a Pt catalyst surface, and a linear relationship between surface coverage and NO_x concentration was observed. On the contrary, the results of Mohtadi et al. [5] showed that the rate of NO_2 poisoning did not strongly depend on NO_2 concentration, suggesting that the NO_2 poisoning did not involve poisoning species on catalyst surface. They speculated that the poisoning species might be NH_4^+ formed through the electrochemical reduction of NO_2, which affected only the ionomer and/or the catalyst–ionomer interface [5]. At the same time, the electrochemical results by Yang et al. [8] even suggested that the impacts of NO_x resulted mainly from the superposition of the oxygen reduction reaction (ORR) and the NO_x oxidation reaction, leading to the increase in cathodic impedance.

From these previous studies, it is clear that the poisoning impact of NO_x is inconsistent. More importantly, the poisoning mechanism of NO_x is still not well understood. A recent review on studies of fuel cell contamination emphasized the urgent need for further understanding of the fundamentals involved in cathode poisoning [9]. Clarifying how air contaminants deactivate the Pt catalyst can help with the development of operational strategies that prevent fuel cells from deactivation, making PEM fuel cell a more robust technology. In addition, although nearly complete recovery of the cell performance was reported to be possible by purging fuel cell

* Corresponding author. Tel.: +86 451 82569890; fax: +86 451 84346500.
** Corresponding author. Tel.: +86 451 86403216; fax: +86 451 86413720.
E-mail addresses: chenmeng@hrbeu.edu.cn (M. Chen), cydu@hit.edu.cn (C. Du).

0378-7753/$ – see front matter © 2010 Elsevier B.V. All rights reserved.
doi:10.1016/j.jpowsour.2010.07.091

with clean air or N_2 [5], efficient recovery methods are still lacking because hours of purging is not really feasible for practical applications, in particular for transportation applications. The purpose of this study was to further elucidate and clarify the poisoning of NO_x on the commonly used Pt/C catalyst. Firstly, the Pt/C catalyst was synthesized by a microwave-assisted polyol method. Then, this catalyst was characterized by transmission electron microscopy (TEM) and X-ray diffraction (XRD). After that, the absorption of NO_x and its poisoning impact on the ORR kinetics was investigated by using a three-electrode cell in a controlled acidic liquid electrolyte. Finally, the recovery of NO_x poisoning through potential sweeping was explored. Using the three-electrode method in our investigation could rule out the interference from the anode and the electrolyte membrane as often encountered in complete fuel cell studies. Moreover, to quantify the ORR kinetics, we used rotating-disk-electrode (RDE) measurement, which permits the correction for diffusion limitation of oxygen in solution and allows isolation of the ORR kinetics [10]. Our method, as far as we know, has never been applied to the poisoning of NO_x on Pt/C catalysts in previous studies, and will give more insightful information on this problem.

2. Experimental

The 40 wt% Pt/C catalyst was synthesized by a microwave-assisted polyol method [11]. Briefly, 40 mg Vulcan XC-72 carbon powder was firstly mixed with 40 ml ethylene glycol (EG) and 10 ml isopropanol to form a homogeneous ink by ultrasonic agitating for 7 h. Then, 3.6 ml 0.038 M H_2PtCl_6 solution was added into the ink drop by drop and the mixture was kept in stirring state for 3 h. After that, pH value of the mixture was adjusted to 12 with 2 M NaOH solution, and the mixture was subsequently subject to microwave-heating for 1 min. After cooling to room temperature, 1 M HNO_3 was used to adjust pH value of the mixture to 3–4, followed with continuous stirring for 3 h. Finally, the catalyst was obtained by washing with boiling deionized water until the pH value of filtrate was close to 7, and drying under vacuum at 80 °C for 12 h.

Particle morphology and size distribution of the obtained Pt/C catalyst were characterized by TEM using a Hitachi model H-800 system operating at 150 kV. The loading of Pt particles was analyzed by energy dispersive X-ray spectroscopy (EDS). The XRD pattern of the Pt/C catalyst was recorded by means of a Rigaku D/Max2500 X-ray powder diffractometer with a Cu Kα source operating at 40 kV.

All electrochemical measurements were conducted using a three-electrode electrochemical cell with 0.1 M $HClO_4$ solution as the electrolyte at room temperature. A Pt foil and an Hg/Hg_2SO_4 electrode served as the counter and reference electrodes, respectively. A thin-film electrode of the Pt/C catalyst was used as the working electrode, which was prepared according to the following procedure [12]: 6.3 mg Pt/C catalyst, 1.30 ml isopropanol, 4.95 ml deionized water, and 0.4 ml 5 wt% Nafion ionomer were firstly mixed and ultrasonically dispersed for 30 min to form a ink; 7.6 μl of the ink was then taken by a pipette and loaded onto a glass carbon RDE with 4 mm diameter; the RDE electrode was finally allowed to dry at room temperature under vacuum. Before each electrochemical measurement, the working electrode was activated by sweeping potential between 0 and 1.2 V (vs RHE) at a scan rate of 50 mV s^{-1} for 50 cycles in a N_2-purged 0.1 M $HClO_4$ solution. The Pt/C catalyst was poisoned by holding the working electrode at a given absorption potential for 5 min in 0.1 M $HClO_4$ solution that was purged with N_2 contaminated by 500 ppm NO_2 at the rate of 100 ml min^{-1} for 20 min. All the CV measurements were performed at a scan rate of 50 mV s^{-1}. For the ORR experiments, linear sweeping voltammetry (LSV) of the RDE was recorded under various rotating rates by scanning the potential from 0.9 to 0.0 V (vs RHE) at a scan rate of 5 mV s^{-1} in an O_2 saturated 0.1 M $HClO_4$ solution.

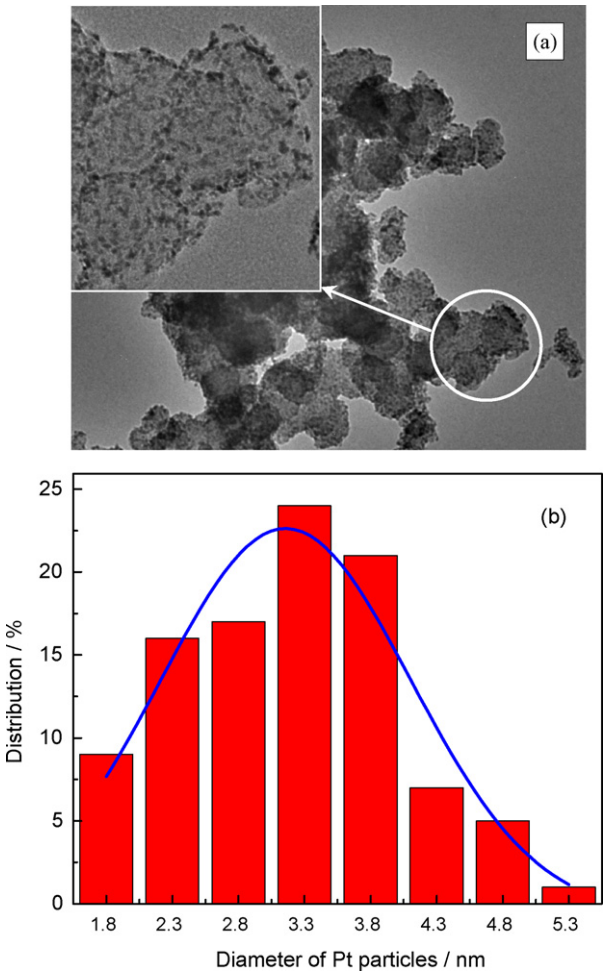

Fig. 1. (a) TEM image of the Pt/C catalyst. Inset: magnified TEM image of the Pt/C catalyst. (b) Histogram of Pt particle size distribution.

3. Results and discussion

3.1. Physical characterization

Fig. 1a shows typical TEM image of the Pt/C catalyst. Apparently, black Pt nanoparticles with small size were evenly dispersed on faint carbon support, although small amount of them aggregated with each other to form slightly larger clusters. The loading of Pt particles was analyzed to be 38.8% by EDS. Fig. 1b gives the distribution of Pt particle diameter estimated from an ensemble of 200 particles in an arbitrarily chosen area of the TEM image. The evaluation of the characteristic diameter of the Pt particles indicated a size distribution from 1.8 to 5.3 nm with an average diameter of 3.1 nm.

In order to obtain the crystalline information of Pt particles, the Pt/C catalyst was characterized by XRD and the result is shown in Fig. 2. Clearly, the XRD pattern exhibited diffraction peaks of (1 1 1), (2 0 0), (2 2 0), and (3 1 1) at 2θ values of 38.75°, 44.43°, 65.42°, and 79.07°, respectively, indicating that Pt was present in the face-centered cubic (fcc) structure [13]. The average crystalline particle size of Pt/C catalysts was 2.93 nm, calculated from the broadening of the (2 2 0) diffraction peak using Scherrer's equation [14]:

$$d = \frac{0.9\lambda}{B\cos\theta} \quad (1)$$

where d is the average crystalline particle size, λ is the wavelength of the X-ray (1.54056 Å), θ is the angle at the maximum of the

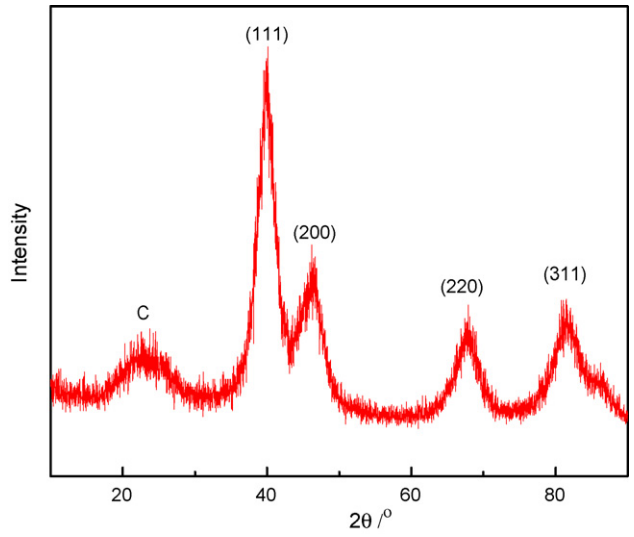

Fig. 2. XRD pattern of the Pt/C catalyst.

peak, and *B* is the width of the peak at half-height. This average size agreed well with the observation in TEM image.

3.2. Electrochemical performance

To evaluate the electrochemical behavior of NO_x on the Pt/C catalyst, the catalyst was firstly poisoned in NO_x-contaminated $HClO_4$ solution by holding at different potentials for 5 min, and then subject to CV sweeping from open circuit potential (OCP) in pure $HClO_4$ solution. Fig. 3a presents the first cycle of CV curves for the poisoned Pt/C catalysts. Apparently, each voltammogram curve showed similar CV features, with a distinct peak at ~1.25 V that was assigned to the oxidation of absorbed NO_x, as well as several other peaks below 1.0 V (these peaks will be discussed in Fig. 3b). The peak at ~1.25 V strongly demonstrated that the poisoning of NO_x was due to the adsorption of NO_x on Pt surface, in consistence with the results in Ref. [7]. In addition, the similar CV features indicated that the absorbed NO_x might be the same for different absorption potentials. It was noteworthy that the peak for NO_x oxidation was almost identical for different poisoned Pt/C catalysts when the absorption potential was below 0.65 V. Nevertheless, as the absorption potential increased above 0.65 V, this peak gradually decreased. The potential of 0.65 V coincided interestingly with the one where platinum started to oxidize (indicated with an arrow in Fig. 3a). This phenomenon suggested that: on the one hand, absorption of NO_x on metallic Pt was probably a chemical rather than an electrochemical process in view of its independence on absorption potential; on the other hand, Pt oxides did not absorb or absorbed less NO_x. This finding might be helpful for alleviating or preventing NO_x poisoning by optimizing operation conditions of the fuel cell cathode. In the following poisoning experiments, if not specifically stated, 0.5 V was chosen as the potential for NO_x absorption.

Fig. 3b shows the sequence of CV curves for the poisoned Pt/C catalyst in pure $HClO_4$ solution. During the first positive sweep from OCP to 1.5 V, the absorbed NO_x was oxidized to NO_3^- and caused a broad peak at ~1.25 V, according to the following equation [6]:

$$NO_x + (3 - x)H_2O \rightarrow NO_3^- + (6 - 2x)H^+ + (5 - 2x)e^- \quad (2)$$

This peak showed an onset potential at ~0.9 V, indicating the NO_x was oxidized above this potential. During the first negative sweep, apparent reduction peaks were observed at ~0.6 V and 0.0–0.3 V. The peak at ~0.6 V mainly resulted from the reduction of Pt oxides formed during the positive sweep. Interestingly, however, this peak

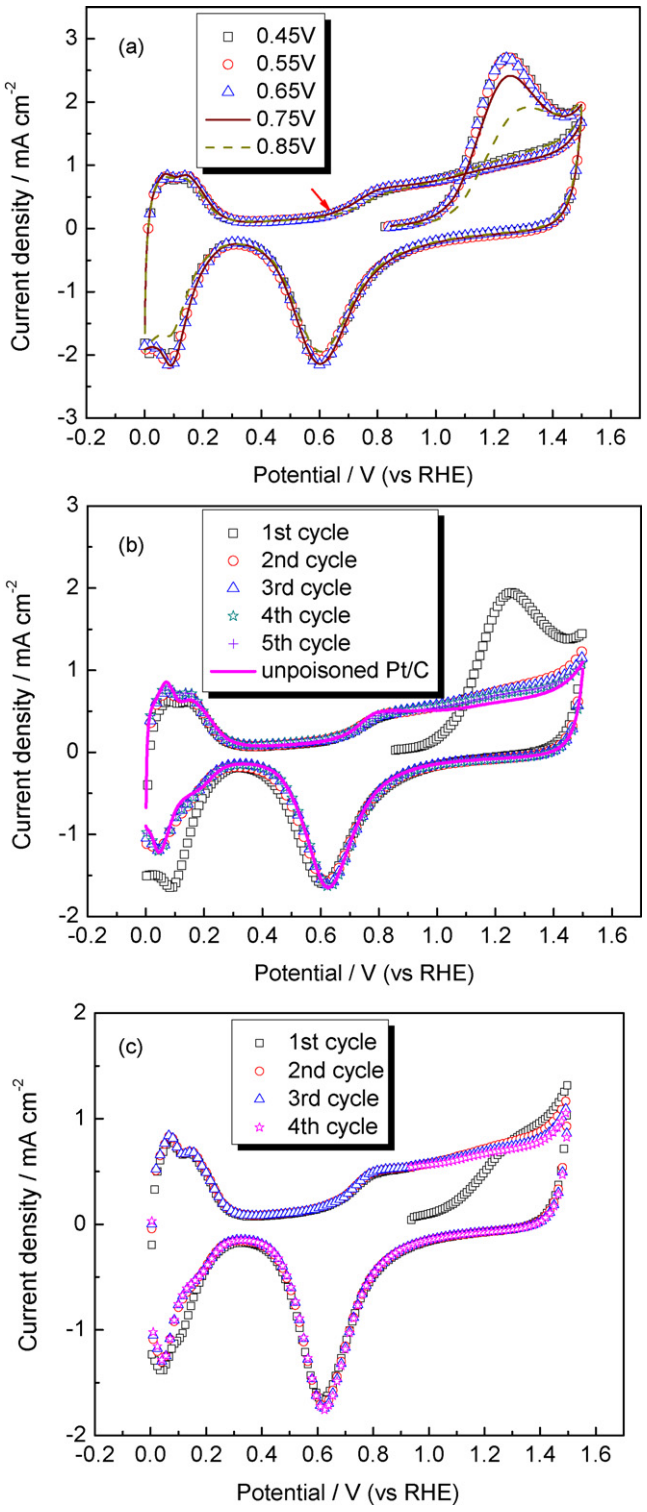

Fig. 3. (a) First voltammetric cycle of the Pt/C catalysts in pure $HClO_4$ solution after poisoned in NO_x-contaminated $HClO_4$ solution by holding at different potentials for 5 min. (b) Sequence of CV curves for the Pt/C catalyst in pure $HClO_4$ solution after poisoned in NO_x-contaminated $HClO_4$ solution at 0.5 V. (c) Sequence of CV curves for the Pt/C catalyst in pure $HClO_4$ solution after submerged in 0.1 M HNO_3 solution for 20 min.

shifted a little negatively in comparison with that of unpoisoned Pt/C, which was possibly caused by the reduction of formed NO_3^- and/or remained NO_x during the positive sweep. The possibility of NO_3^- reduction was verified by CV curves of the Pt/C catalyst after submerged in HNO_3 solution (Fig. 3c), where a slight neg-

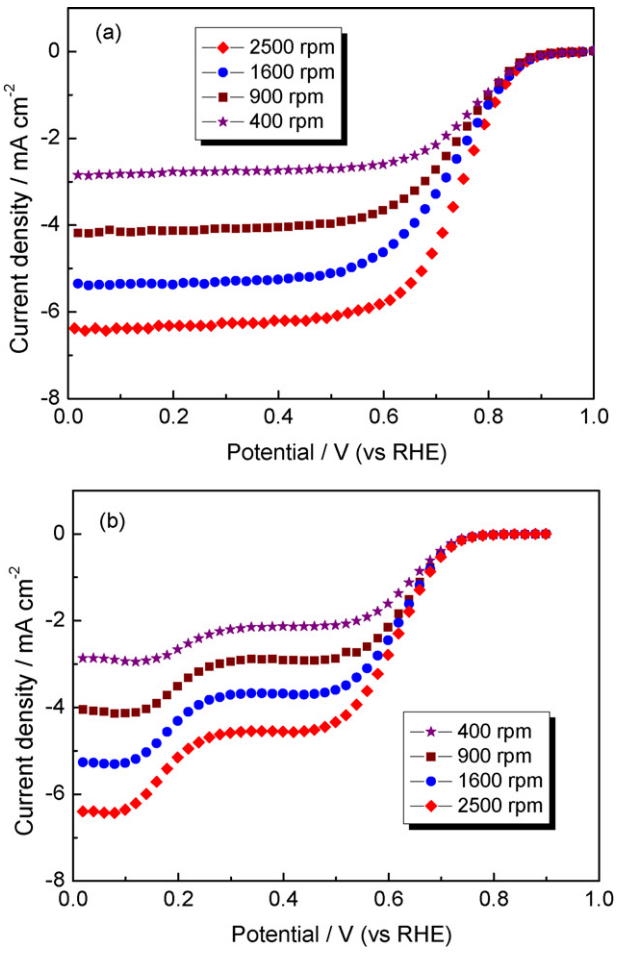

Fig. 4. Linear sweeping voltammetry curves of (a) the unpoisoned and (b) the poisoned Pt/C catalysts in 0.1 M $HClO_4$ solution saturated with O_2 as a function of the RDE rotating rate.

ative shift was also observed for the peak at ~0.6 V. The second peak at 0.0–0.3 V was in hydrogen absorption region, but its value was significantly higher than that for unpoisoned Pt/C. This result was completely different from the case of sulfur oxides poisoning, where a reduced hydrogen absorption peak was observed [15,16], indicating that this peak corresponded not only to the hydrogen absorption, but to the reduction of NO_x that adsorbed on Pt surface based on the following reaction [17]:

$$NO_x + (4+2x)H^+ + (3+2x)e^- \rightarrow NH_4^+ + xH_2O \quad (3)$$

Upon the first positive sweep from 0.0 V to OCP in Fig. 3b, the oxidation peak at 0.0–0.3 V was due to the hydrogen desorption. This peak was less than that of unpoisoned Pt/C, because the absorbed NO_x lowered the Pt surface available for hydrogen absorption. The subsequent broad oxidation peak from ~0.65 V was assigned to the oxidation of Pt. As the cycling number increased, the peak for the oxidation of absorbed NO_x quickly disappeared. Simultaneously, current densities for the hydrogen adsorption/desorption as well as Pt oxidation and its reduction approached rapidly to the unpoisoned values. Within the five cycles, the CV profiles reached a steady state, indicating that the absorption of NO_x on Pt surface was not strong, consistent with the observation in complete fuel cell studies [7,8].

To evaluate the effect of NO_x poisoning on ORR kinetics, the LSV curves of the poisoned and unpoisoned Pt/C catalysts for the ORR as a function of RDE rotating rate are shown in Fig. 4. The unpoisoned Pt/C catalyst (Fig. 4a) gave typical ORR LSV curves on Pt surface, which exhibited onset currents at ~0.90 V and attained diffusion-limited currents at ~0.55 V. For the poisoned Pt/C catalyst (Fig. 4b), however, the onset potential for ORR shifted significantly to <0.75 V. The current density at 0.85 V, where the ORR is almost kinetics-controlled [18], was 0.38 and 0.0055 mA cm^{-2} for the unpoisoned and poisoned catalysts, respectively. This surprising 98.5% decrease of the ORR activity clearly demonstrated the Pt/C catalyst could be significantly poisoned by the absorption of NO_x. At the same time, it was very interesting that the poisoned Pt/C catalyst exhibited two diffusion-controlled plateaus at potentials of 0.25–0.5 V and <0.15 V. This phenomenon was not reported in previous studies concerning NO_x poisoning [2,4–9], and was also highly different from the case of sulfur oxides poisoning [10], where only one diffusion-limited current plateau was observed. Apparently, this difference resulted from the nature of the NO_x absorbed on Pt surface, and might be explained as follows. Initially, the absorbed NO_x notably decreased the active Pt available for the ORR, and thus reduced the diffusion-limited current and formed the plateau at 0.25–0.5 V by lowering the active electrode area (A) and/or the number of transferred electron (n) based on the equation [19]:

$$i_d = 0.62\, nFAD^{2/3}\omega^{1/2}\nu^{-1/6}c^* \quad (4)$$

where i_d is the diffusion-limited current, F is the Faraday constant, D is the diffusion coefficient of O_2, ω is electrode rotation rate in unit of rpm, ν is kinematic viscosity of water, and c^* is the concentration of O_2 in dilute $HClO_4$ solution. Along with the negatively sweeping potential, NO_x was gradually reduced to NH_4^+ according to Eq. (3). NH_4^+ was then dissolved into the solution and left more active Pt surface, which increased the diffusion-limited current. When most of the NO_x was reduced, the active surface area of Pt reached a steady value, forming the other diffusion-limited current plateau at <0.15 V. For sulfur oxides poisoning, however, although sulfur oxides could also be reduced, their reduction product was sulfur and could not be removed from the electrode, leading to only one diffusion-limited current as revealed in Ref. [10]. The above results clearly demonstrated that the poisoning of NO_x was both severe and unique.

Fig. 5a and b shows Koutecky–Levich (K–L) plots ($1/j$ vs $1/\omega^{0.5}$) as a function of potential for the unpoisoned and poisoned Pt/C catalysts, respectively. It could be seen that all the K–L plots exhibited a linear relationship between $1/j$ and $1/\omega^{0.5}$, indicating that the ORR process on both unpoisoned and poisoned Pt/C catalysts followed the K–L equation. We compared the slopes of these K–L plots with the theoretically calculated values for the four-electron oxygen reduction using the K–L equation [19]:

$$\frac{1}{j} = \frac{1}{j_k} + \frac{1}{j_d} = \frac{1}{j_k} + \frac{1}{0.62\ nFD^{2/3}\omega^{1/2}\nu^{-1/6}c} = \frac{1}{j_k} + \frac{1}{B\omega^{1/2}}$$

$$\text{with} \quad B = 0.62\, nFD^{2/3}\nu^{-1/6}c^* \quad (5)$$

where j is the measured current density, j_k is the kinetic current density, and j_d is the diffusion-limited current density. From the slopes of these K–L plots, the B values were obtained for the unpoisoned and NO_x poisoned Pt/C catalysts, respectively. The theoretical calculated B value for a four-electron ($n = 4$) process is 2.41×10^{-2} mA cm^{-2} $rpm^{-0.5}$ by using the parameters ($D = 1.93 \times 10^{-5}$ cm^2 s^{-1}, $\nu = 1.01 \times 10^{-2}$ cm^2 s^{-1}, and $c^* = 1.26 \times 10^{-6}$ mol cm^{-3}). Thus, the nominal n values for the unpoisoned and poisoned Pt/C catalysts were calculated and the results are presented in Fig. 5c. Nominal n values essentially assume that all the electrochemical active surface area could catalyze the ORR, so that if some surface area was poisoned by NO_x, the real current for ORR would decrease, leading to reduced nominal n values. Clearly, the measured nominal n values for the unpoisoned Pt/C catalyst agreed well with the theoretical value, meaning that

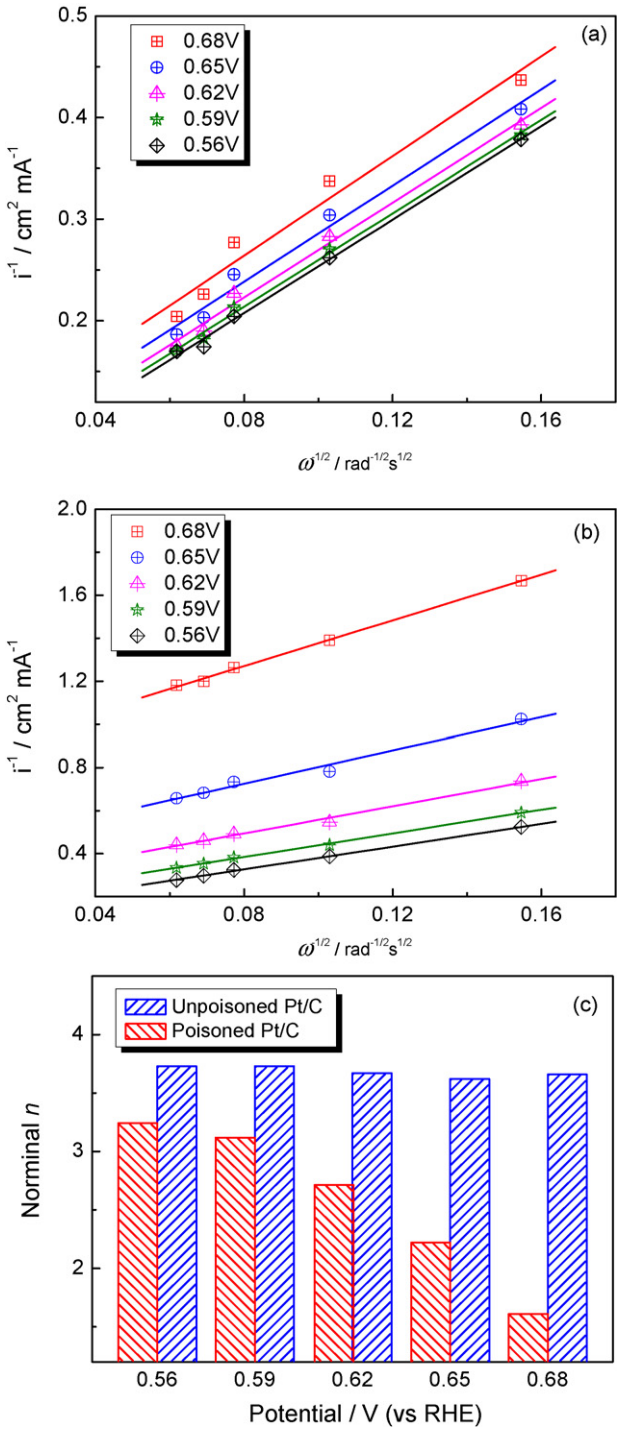

Fig. 5. Koutecky–Levich plots for oxygen reduction on (a) the unpoisoned and (b) the poisoned Pt/C catalysts in an O_2 saturated 0.1 M $HClO_4$ solution at various potentials. (c) Norminal number of transferred electron during the ORR calculated from Koutecky–Levich plots as a function of potential.

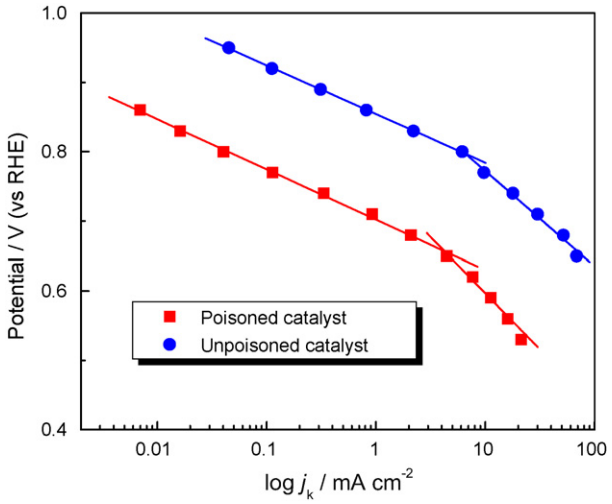

Fig. 6. Tafel curves of the unpoisoned and poisoned Pt/C catalysts.

the number of electrons involved in the ORR was almost four, and thus the predominant product was water. In comparison, however, the nominal n values for the poisoned Pt/C were significantly decreased, confirming the significant poisoning of NO_x on the Pt/C catalyst. Moreover, this decrease became more remarkable at higher potentials for the practical operation potential range of cathode (0.5–0.7 V), which might be attributed to more severe NO_x poisoning at higher potentials because NO_x could be reduced at lower potentials. This result implied a likely route to alleviate the poisoning of NO_x by properly reducing the operating potential (i.e., increasing the working current density).

To further clarify the poisoning mechanism of NO_x, the kinetic current density (j_k) was obtained by extrapolation of the K–L plots for $\omega^{-1/2} \rightarrow 0$. Fig. 6 gives the Tafel curves by plotting $\log j_k$ vs electrode potential for the unpoisoned and poisoned Pt/C catalysts. The polarization current density for poisoned Pt/C catalyst was much lower than that for unpoisoned one, which was consistent with the nominal n values in Fig. 5c, suggesting the significant poisoning of NO_x on Pt/C catalyst. Both Tafel curves exhibited two distinct slopes at low and high current densities (70 and 138 mV dec^{-1} for unpoisoned Pt/C; 72 and 151 for poisoned Pt/C), which agreed well with the values for Pt based catalysts reported in the literature [20,21]. The existence of two slopes could be explained by the coverage of the catalyst surface with absorbed oxygen species, which followed a Temkin isotherm at low current densities and a Langmuir isotherm at high current densities [21,22]. The similar Tafel slope values for the unpoisoned and poisoned Pt/C catalysts indicated the absorption conditions were the same for both catalysts. Thus, the ORR mechanism remained unchanged after the poisoning of NO_x, in despite of the lower nominal n values due to the absorption of NO_x. This meant that the poisoning of NO_x was just associated with the reduction of electrochemically active surface area, rather than the change of the ORR kinetics.

In view of the severe poisoning of NO_x on Pt/C catalyst, it is essential to search for the efficient recovery method after the NO_x poisoning. Firstly, we studied the reduction removal of the absorbed NO_x. Fig. 7a presents the first several cycles of potential sweeping curves for the poisoned Pt/C catalyst in the N_2-purged 0.1 M $HClO_4$ solution between 0.0 V and OCP, where reduction of the absorbed NO_x happened. The curve for the unpoisoned Pt/C is also shown as a reference. Similarly to those shown in Fig. 3, the absorbed NO_x significantly changed the CV characteristics of the Pt/C catalyst. During the first negative sweep, a broad reduction peak appeared, due to the NO_x reduction as well as the hydrogen absorption. This peak was significantly larger than that of unpoisoned Pt/C, indicating that considerable NO_x absorbed on Pt surface. During the first positive sweep, the peak for hydrogen desorption was relatively small due to the presence of absorbed NO_x. In the subsequent cycles, the reduction peak decreased notably, while the oxidation peak increased. Within five cycles, the two peaks became stable. Using the data in Fig. 7a, the anodic and cathodic charges were calculated by integrating the positive and negative sweeping peaks for each cycle, and the results are plotted in Fig. 7b. Appar-

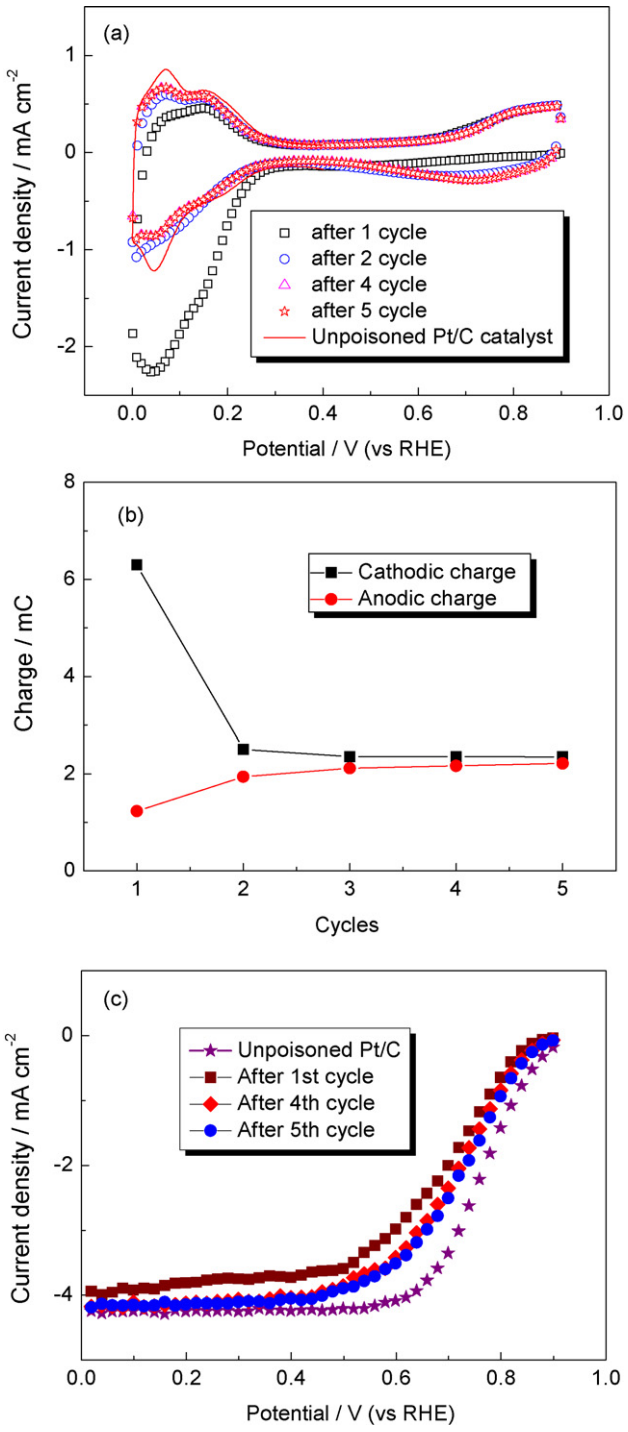

Fig. 7. (a) Potential sweeping curves for the poisoned Pt/C catalyst in the N_2-purged 0.1 M $HClO_4$ solution between 0.0 V and open circuit potential. (b) Anodic and cathodic charges evolution during reduction recovery as a function of the cycle number. (c) Linear sweeping voltammetry curves of the reduction-recovered Pt/C catalyst in 0.1 M $HClO_4$ solution saturated with O_2 at a rotating rate of 1600 rpm.

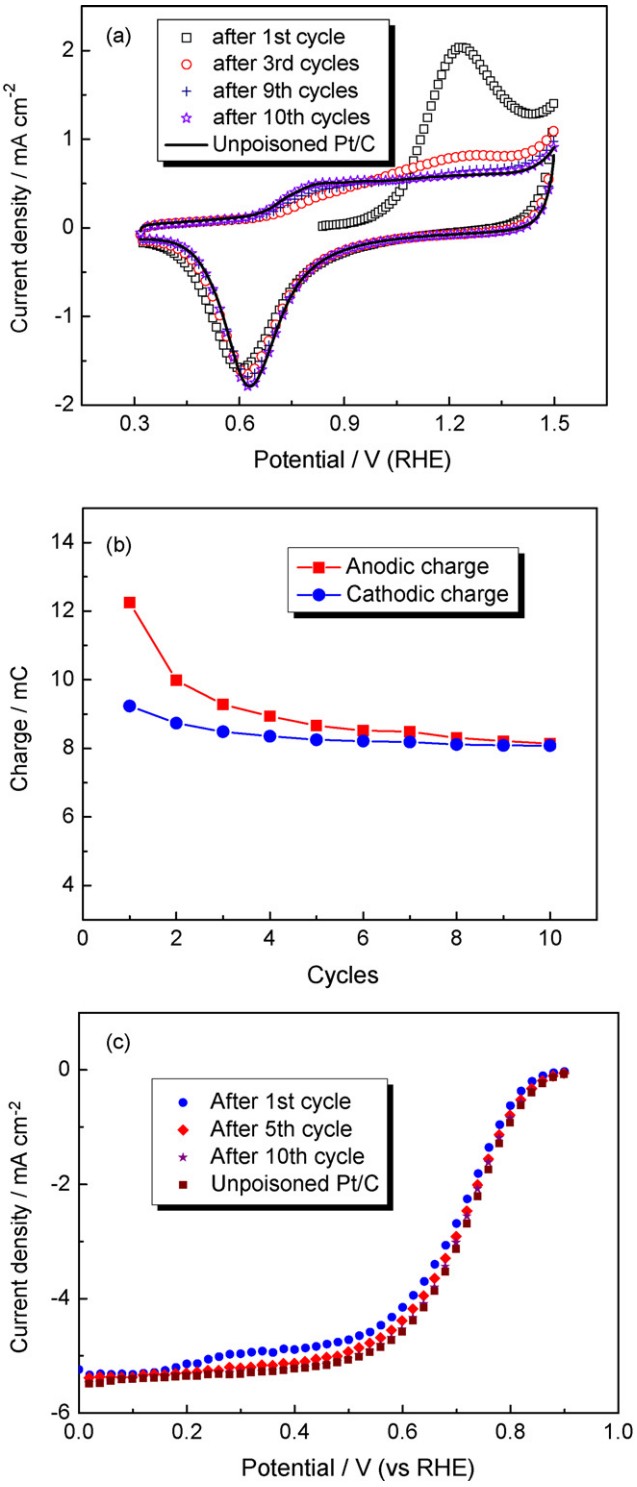

Fig. 8. (a) Potential sweeping curves for the poisoned Pt/C catalyst in the N_2-purged 0.1 M $HClO_4$ solution. (b) Anodic and cathodic charges evolution during oxidation recovery as a function of the cycle number. (c) Linear sweeping voltammetry curves of the oxidation recovered Pt/C catalyst in 0.1 M $HClO_4$ solution saturated with O_2 at a rotating rate of 1600 rpm.

ently, the anodic and cathodic charges quickly approached to each other and almost converged at the fifth cycle. This result implied that the reduction removal of absorbed NO_x was essentially finished during the first several potential cycles. However, it had to be mentioned that even after several cycles of the reduction removal, the hydrogen absorption/desorption peaks for the poisoned catalyst could not be thoroughly recovered to that of unpoisoned one. Two reasons might be responsible for this phenomenon: one was that the absorbed NO_x could be difficult to be completely reduced as revealed in Ref. [23]; the other was that the formed NH_4^+ affected the ionomer and/or the catalyst–ionomer interface, because NH_4^+ was identified as a poisoning species for Nafion ionomer [24]. Fig. 7c gives RDE LSV curves of the ORR for the poisoned Pt/C catalyst that was reduction-recovered for different cycles. Apparently, after the

first cycle of reduction recovery, the ORR behavior of the poisoned Pt/C catalyst exhibited only one diffusion-limited current density region, which was similar to that of the unpoisoned one, suggesting that the Pt/C catalyst was greatly recovered. After five cycles of potential sweeping, the LSV ORR curves were almost unchanged. However, the ORR activity of the poisoned Pt/C catalyst was still inferior to that of the unpoisoned, even after several cycles of reduction removal of NO_x. This indicated that the ORR activity of the poisoned Pt/C catalyst could not be recovered by only reduction removal, which was consistent with the results in hydrogen absorption/desorption in Fig. 7a.

Fig. 8a shows the CV curves of the poisoned Pt/C catalyst in the N_2-purged 0.1 M $HClO_4$ solution between 0.32 and 1.5 V, where oxidation of the absorbed NO_x mainly happened. During the first positive sweep, the oxidation of the adsorbed NO_x to NO_3^- led to the broad anodic peak at ~1.25 V. During the first negative sweep, the reduction current peak at ~0.6 V was mainly due to the reduction of Pt oxides. With increase in the cycle number, the oxidation peak quickly decreased, indicating that the NO_x species were easily removed from the Pt/C surface by oxidation recovery. After 10 cycles, the CV was essentially identical to that of an unpoisoned Pt/C. This result suggested that the NO_x removal through oxidation was more efficient than that through reduction. This might be due to that the absorbed NO_x was more easily to be oxidized, or that the oxidized NO_3^- dissolved easily into solution and did not affect the ionomer and/or the catalyst–ionomer interface as NH_4^+. The anodic and cathodic charges for each cycle (Fig. 8b) showed that 10 oxidative sweeps were necessary for the anodic and cathodic charges to converge, indicating that the NO_x species were completely removed. Fig. 8c presents the ORR LSV curves for the poisoned Pt/C catalyst that was oxidation recovered for different cycles. Clearly, the LSV curve for the poisoned Pt/C catalyst coincided with that of unpoisoned one after 10 cycles, suggesting that the Pt/C catalyst was completely recovered, in consistent with the results in Fig. 8a and b.

4. Conclusions

Rotating-disk-electrode (RDE) measurements in a three-electrode electrochemical cell have been performed to study the poisoning of NO_x contaminants on Pt/C catalysts. Using the three-electrode method could rule out the interference from the anode and the electrolyte membrane. Moreover, RDE measurements permit the correction for diffusion limitation of oxygen and allow isolation of the ORR kinetics. It has been found that the absorption of NO_x on metallic Pt is more significant than on Pt oxides, and this absorption is mainly a chemical process. In addition, although the absorption of NO_x on Pt surface is not strong, exposure to NO_x contaminants can result in significant performance degradations of Pt/C catalysts. At the same time, in despite of the rather complex process, it seems that the ORR mechanism remains unchanged after the NO_x poisoning, because similar Tafel slopes have been observed for the unpoisoned and poisoned Pt/C catalysts. This indicates that the NO_x poisoning on Pt/C catalysts is just due to the reduction of electrochemically active surface area. Since lower potentials facilitate the reduction of NO_x to water soluble NH_4^+, reducing the working potential might mitigate the poisoning of NO_x. However, the performance loss due to the NO_x poisoning can be completely recovered by the oxidation removal, but not by the reduction removal mode.

Acknowledgements

This work was supported by the National Science Foundation of China under contract No. 20706010 and 20876029, the Harbin Talents Foundation in the Innovation of Science and Technology under contact No. 2008RFQXG059, and the Natural Scientific Research Innovation Foundation in Harbin Institute of Technology.

References

[1] R. Borup, J. Meyers, B. Pivovar, Y. Kim, R. Mukundan, N. Garland, D. Myers, M. Wilson, F. Garzon, D. Wood, P. Zelenay, K. More, K. Stroh, T. Zawodzinski, X. Boncella, J. McGrath, O. Inaba, K. Miyatake, M. Hori, K. Ota, Z. Ogumi, S. Miyata, A. Nishikata, Z. Siroma, Y. Uchimoto, K. Yasuda, K. Kimijima, N. Iwashita, Chem. Rev. 107 (2007) 3904.
[2] Y. Nagahara, S. Sugawara, K. Shinohara, J. Power Sources 182 (2008) 422.
[3] B. Gould, O. Baturina, K. Swider-Lyons, J. Power Sources 188 (2009) 89.
[4] J. Moore, P. Adcock, J. Lakeman, G. Mepsted, J. Power Sources 85 (2000) 254.
[5] R. Mohtadi, W. Lee, J. Van Zee, J. Power Sources 138 (2004) 216.
[6] F. Jing, M. Hou, W. Shi, J. Fu, H. Yu, P. Ming, B. Yi, J. Power Sources 166 (2007) 172.
[7] S. Knights, N. Jia, C. Chuy, J. Zhang, Fuel Cell Seminar 2005: Fuel Cell Progress, Challenges and Markets, Palm Prings, California, 2005.
[8] D. Yang, J. Ma, L. Xu, M. Wu, H. Wang, Electrochim. Acta 51 (2006) 4039.
[9] X. Cheng, Z. Shi, N. Glass, L. Zhang, J. Zhan, D. Song, Z. Liu, H. Wang, J. Shen, J. Power Sources 165 (2007) 739.
[10] Y. Garsany, O. Baturina, K. Swider-Lyons, J. Electrochem. Soc. 156 (2009) B848.
[11] W. Chen, J. Lee, Z. Liu, Chem. Commun. 21 (2002) 2588.
[12] T. Schmidt, H. Gasteiger, G. Stäb, P. Urban, D. Kolb, R. Behm, J. Electrochem. Soc. 145 (1998) 2354.
[13] J. Xu, K. Hua, G. Sun, C. Wang, X. Lv, Y. Wang, Electrochem. Commun. 8 (2006) 982.
[14] Z. Liang, T. Zhao, J. Phys. Chem. C 111 (2007) 8128.
[15] Y. Zhai, G. Bender, S. Dorn, R. Rocheleau, J. Electrochem. Soc. 157 (2010) B20.
[16] Y. Garsany, O. Baturina, K. Swider-Lyons, J. Electrochem. Soc. 154 (2007) B670.
[17] A. de Vooys, G. Beltramo, B. van Riet, J. van Veen, M. Koper, Electrochim. Acta 49 (2004) 1307.
[18] W. Chen, J. Kim, S. Sun, S. Chen, J. Phys. Chem. C 112 (2008) 3891.
[19] N. Markovic, H. Gasteiger, B. Grgur, P. Ross, J. Electroanal. Chem. 467 (1999) 157.
[20] T. Toda, H. Igarashi, H. Uchida, M. Watanabe, J. Electrochem. Soc. 146 (1999) 3750.
[21] V. Stamenkovic, T. Schmidt, P. Ross, N. Markovic, J. Phys. Chem. B 106 (2002) 11970.
[22] N. Elezović, B. Babić, L. Vračar, J. Krstajić, J. Serb. Chem. Soc. 72 (2007) 699.
[23] C. Lin, W. Hung, C. Wu, K. Ho, Sens. Actuators B 136 (2009) 32.
[24] F. Uribe, S. Gottesfeld, T. Zawodzinski, J. Electrochem. Soc. 149 (2002) A293.